Technical Report

Joining Technology That Contributes to Improving the Reliability of Next-generation EV Body

Tohru OKADA*
Taiga TANIGUCHI
Junichiro SUZUKI
Masatoshi TOKUNAGA
Hiroshi YOSHIDA
Hiroshi HORIKAWA
Takumi MIZUTANI
Takahiro AITO
Hiroki FUJIMOTO

Abstract

To fully exploit the performance of high-strength steel sheets and realize high-performance automobile bodies, preventing fracture of spot-welded joints is a key enabling technology. Effective countermeasures require (i) accurate assessment of the loads acting on spot welds in real vehicles and (ii) robust fracture prediction based on that assessment. In this report, we present a case study in which the effectiveness of several countermeasures for spot-weld fracture in a component was verified using Nippon Steel Corporation's proprietary spot-weld fracture prediction software, NSafe™-SPOT. By identifying and limiting the locations where countermeasures are necessary through high-accuracy fracture prediction, process time and cost increases can be minimized, thereby contributing to the development of automobile bodies with excellent crash performance.

1. Introduction

Achieving carbon neutrality by 2050 requires reducing greenhouse-gas emissions, including CO_2, across the entire product lifecycle. In the automotive sector, the adoption of battery electric vehicles (BEVs), which emit minimal greenhouse gases during operation, has accelerated rapidly in recent years.[1)] However, BEV battery packs typically weigh several hundred kilograms, significantly increasing vehicle mass. Consequently, vehicle body structures must satisfy more stringent crash performance requirements than ever before.

During crash events, fracture of the base material or failure of spot-welded joints may occur, preventing achievement of the intended design performance. **Figure 1** shows the relationship between base-material strength and (i) tensile shear strength (TSS), an index for shear loading in spot-welded joints, and (ii) cross tensile strength (CTS), an index for axial (peel) loading. TSS decreases when base-material strength exceeds the 1.5 GPa class, and CTS shows a decreasing trend when base-material strength exceeds the 590 MPa class.[2)] With the rapid expansion of ultra-high-strength steel sheet applications in recent years, robust spot-weld design has become increasingly challenging. Therefore, countermeasures to prevent spot-weld fracture are a key technology for enhancing auto-

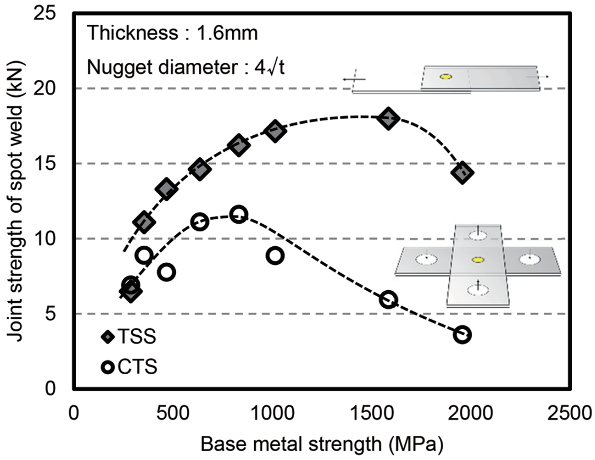

Fig. 1 Relationship between spot weld joint strength and base metal strength

* Ph.D., Senior Manager, Head of Section, Welding & Joining Research Lab., Steel Research Laboratories
20-1 Shintomi, Futtsu City, Chiba Pref. 293-8511

mobile body performance.

To implement appropriate countermeasures, it is important to predict fracture in advance using finite element method (FEM) analysis. Nippon Steel Corporation has developed and implemented NSafe™-SPOT (spot-weld fracture prediction software) and NSafe™-MAT (material fracture prediction software).[3–5] These tools are intended for full-vehicle crash models and run as user subroutines in LS-DYNA, a widely used general-purpose solver for automotive crash analysis.

This report introduces a joining-solution case study in which countermeasures were applied to locations with a high risk of spot-weld fracture based on NSafe™-SPOT predictions, thereby improving component performance.

2. Spot Weld Fracture Prediction Technology

As noted above, NSafe™-SPOT was developed for full-vehicle crash models. Structural members are modeled using relatively coarse shell elements, while spot welds are modeled using beam elements (which can be treated as solid equivalents via an LS-DYNA option during calculation). When spot welds are modeled as beam elements in LS-DYNA, the loads at the welds are output as shear force, axial force, and bending moment. These correspond to TSS, CTS, and L-shaped tensile strength (LTS), respectively, which are commonly used indices of spot-weld joint strength. In real vehicles, however, spot welds experience mixed-mode loading, and the fracture limit varies with steel grade, sheet thickness, welding conditions, and member geometry. This complexity makes it difficult to build a practical predictive model if all factors are treated independently.

Accordingly, Nippon Steel conducted systematic experiments in which material, spot-welding conditions, and specimen width were varied using TSS, CTS, and LTS tests. By evaluating the shear force, axial force, bending moment, and their resultant acting on the spot weld, it was found that—even under identical material and welding conditions—the fracture strength changes with specimen width. Based on these findings and a stress-concentration concept, the relationship between the stress concentration factor and the ratio of nugget diameter to specimen width was organized, enabling spot-weld fracture to be predicted using a single fracture-limit curve irrespective of steel grade, sheet thickness, welding conditions, specimen width, or loading mode (TSS/CTS/LTS).

Because generating input data for thousands of spot welds is a substantial task, NSafe™-SPOT Pre was also developed to support model preparation. NSafe™-SPOT Pre enables fracture criteria to be generated for each spot weld based on its specific attributes: steel grade, sheet thickness, nugget diameter, and member geometry. Here, the relevant geometric attribute is the width over which each spot weld carries load (hereafter, the effective width). Specifically, it corresponds to spot pitch or flange width perpendicular to the load direction (in joint tests, it corresponds to specimen width). A distinctive feature of NSafe™-SPOT compared with other prediction approaches is that the effective width is explicitly included in the fracture criterion. This allows fracture prediction that reflects the actual joint-surface geometry in real components.

A case study comparing predictions with fracture observed in full-vehicle offset frontal crash tests, focusing on the floor and dashboard panel joint region, has been reported.[6] Good agreement was obtained, and it was shown that detailed time-history analysis of the loading state at each weld is possible, enabling use in root-cause analysis and countermeasure design.

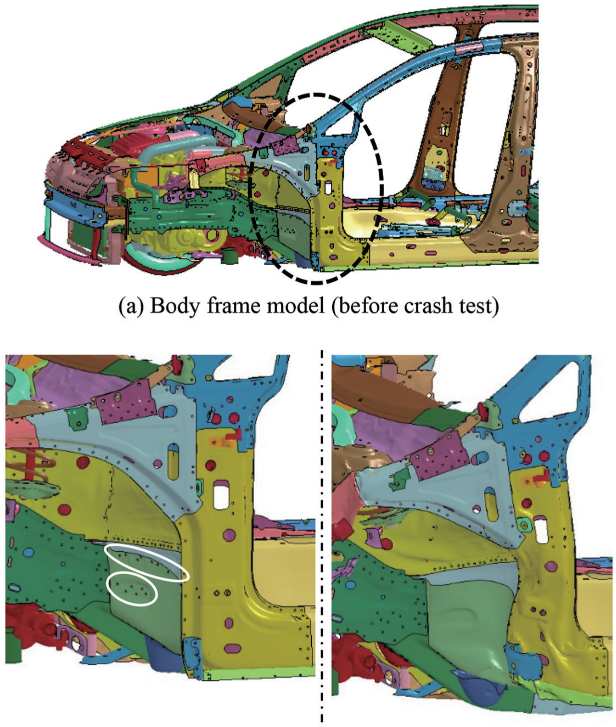

(a) Body frame model (before crash test)

(b1) Initial state (b2) 50ms

Fig. 2 Deformation during vehicle crash test and fracture prediction results for spot welds

Figure 2 shows an example of spot-weld fracture prediction for a small-overlap frontal crash using a full-vehicle model. For the A-pillar lower and dash-panel joint region highlighted by dashed lines in the body-skeleton view (Fig. 2(a)), comparison of the initial state (0 ms) and the state near maximum deformation (50 ms) confirms that the spot welds on the dash panel (circled) fracture and undergo large deformation by 50 ms. As the influence of spot-weld fracture on body performance increases, the system continues to improve prediction accuracy through functional enhancements and by accommodating new steel grades.

3. Spot Weld Fracture Countermeasure Technology

3.1 Spot design

Well-known approaches to suppress spot-weld fracture include dispersing load by reducing spot pitch and increasing nugget diameter. Although effective, these measures may be insufficient when load concentrates locally at specific welds, when fracture occurs in high-carbon steel sheets where the benefit of increasing nugget diameter is relatively small, or when maintaining consistent nugget diameter is difficult in production.

The following sections describe two countermeasure processes that can be selected depending on the fracture mode and production constraints.

3.2 Combination of spot welding and laser welding

Spot welding forms discrete point joints, and peel loading can act on the joint region through gaps between weld points. In such cases, continuous welding is effective; however, laser welding—one representative continuous joining method—has limited tolerance to gaps between sheets. This can lead to defects such as underfill and blowholes, and may also cause dimensional-accuracy issues due to thermal distortion.

To address these issues, we developed a method in which laser welding is applied over spot welds after spot-weld assembly. By using spot welding to control inter-sheet gaps to below a specified level, stable laser welding becomes possible. **Figure 3** shows the appearance and cross-sectional images of a specimen laser-welded after spot welding (cross sections were taken perpendicular to the laser-weld line). A stable laser-welded joint without defects is observed. This method preserves the structural strength achieved by spot-weld assembly while simultaneously suppressing peel loading at the spot welds by bridging the gaps between weld points. In addition, the increased bonded area provided by laser welding contributes to fracture suppression under shear loading. Effectiveness in suppressing fracture in the softened heat-affected zone (HAZ) under in-plane tensile loading has also been reported.[2, 7)]

This technology can be implemented by replacing part of a body production line—typically consisting mainly of spot welders—with laser welding equipment. In addition, some in-service production lines install laser welding stations downstream of spot welding.[8)] In such cases, closed-section structures (e.g., from the A-pillar to the roof rail) may already include laser welds to enhance stiffness. As shown in **Fig. 4**, by applying laser welding not only at existing laser-weld locations but also across selected spot-weld locations, spot-weld fracture countermeasures can be achieved without additional equipment investment.

3.3 Adaptive control post-heating

Various post-heating techniques have been proposed to improve the joint strength of spot welds.[9–11)] Examples include approaches to mitigate solidification segregation (P and S), which reduces peel strength, and approaches to improve toughness by annealing the nugget. However, for steels with higher carbon content, the benefit of segregation mitigation decreases. For steel sheets with carbon content exceeding 0.3%, post-heating (tempering) is particularly effective for improving joint strength.

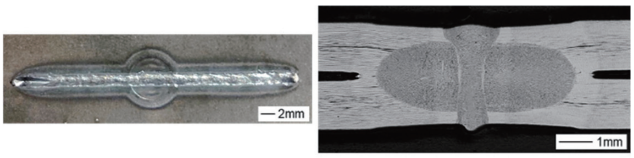

Fig. 3 Appearance and cross section images of spot and laser welded joint

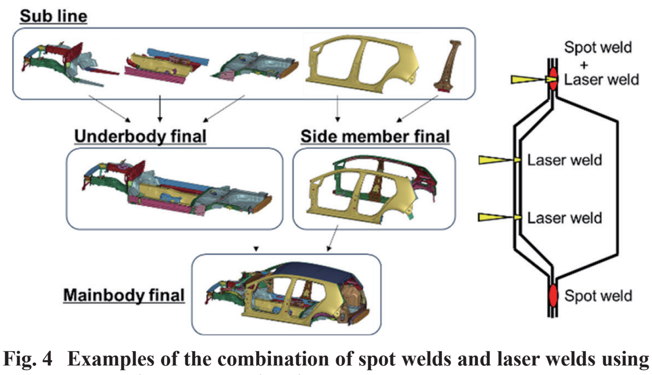

Fig. 4 Examples of the combination of spot welds and laser welds using conventional production line

Post-heating is a long-established technique, but practical challenges have limited its use in mass production: low robustness to production disturbances,[12)] a narrow process window,[13)] and insufficiently established quality-control methods.

Nippon Steel developed a method that improves robustness by applying adaptive control to post-heating. Adaptive control monitors weld-quality-related parameters during welding and uses the measurements for real-time feedback control. Inter-electrode resistance, which is relatively easy to measure, is typically used. Under predetermined reference conditions, a time-history characteristic (hereafter, the master curve) is obtained, and heat input is controlled to reproduce this master curve.

After storing the master curve for the post-heating stage, the stability of the tempering effect with and without adaptive control was examined for multiple nugget diameters. Nugget diameter variation was simulated by changing the main welding current, reflecting variation expected in mass production. **Figure 5** shows the current waveforms and the hardness distributions in the spot-weld region.

Without adaptive control (Fig. 5(a)), the post-heating current remained constant irrespective of the main welding current (i.e., nugget diameter), and the hardness distribution varied substantially with nugget diameter. With adaptive control (Fig. 5(b)), the post-heating current was automatically reduced for smaller nugget diameters and increased for larger nugget diameters, and the hardness distribution remained essentially constant. This demonstrates that the method enables appropriate and stable tempering at the nugget edge. Nippon Steel also developed a method to evaluate tempering effectiveness based on the resistance waveform during post-heating, thereby establishing techniques to address key challenges for mass-production implementation.

4. Component Verification Results

In this study, an A-pillar prototype was fabricated with a Al-coated 2.0 GPa-class steel sheet (1.6 mm thickness) for the outer member and an Al-coated 1.5 GPa-class steel sheet (1.2 mm thickness) for the inner member. The effectiveness of the spot-weld fracture countermeasures described in Section 3 was verified via a crush test simulating an offset frontal crash.

A schematic of the A-pillar crush test is shown in **Fig. 6**. Nippon Steel has established boundary conditions for partial models that reproduce full-vehicle loading modes through analysis, developed multifunctional crash-test techniques to realize these conditions, and accumulated relevant know-how.

The baseline assembly condition used a nugget diameter of $4\sqrt{t}$ and a spot pitch of 30 mm (t: sheet thickness). **Figure 7** compares NSafe™-SPOT predictions of spot-weld fracture under the baseline condition with experimental observations. The analysis indicated that buckling of the sheet between spot welds on the compression side of the A-pillar bend caused adjacent spot welds to fracture under an LTS-dominant loading mode. In the experiment, the locations where fracture initiated matched the predicted locations. Subsequently, fracture propagated to surrounding welds, confirming that NSafe™-SPOT captured the actual phenomenon with high fidelity.

Based on these results, several countermeasures were applied to the region containing the two initial fracture sites and their neighboring spot welds, and component performance was evaluated. The investigated conditions were: (i) increasing nugget diameter to $5\sqrt{t}$, (ii) applying adaptive-control post-heating, and (iii) adding laser welds between spot welds centered on the nuggets. **Figure 8** compares the maximum load for each assembly condition. Under the

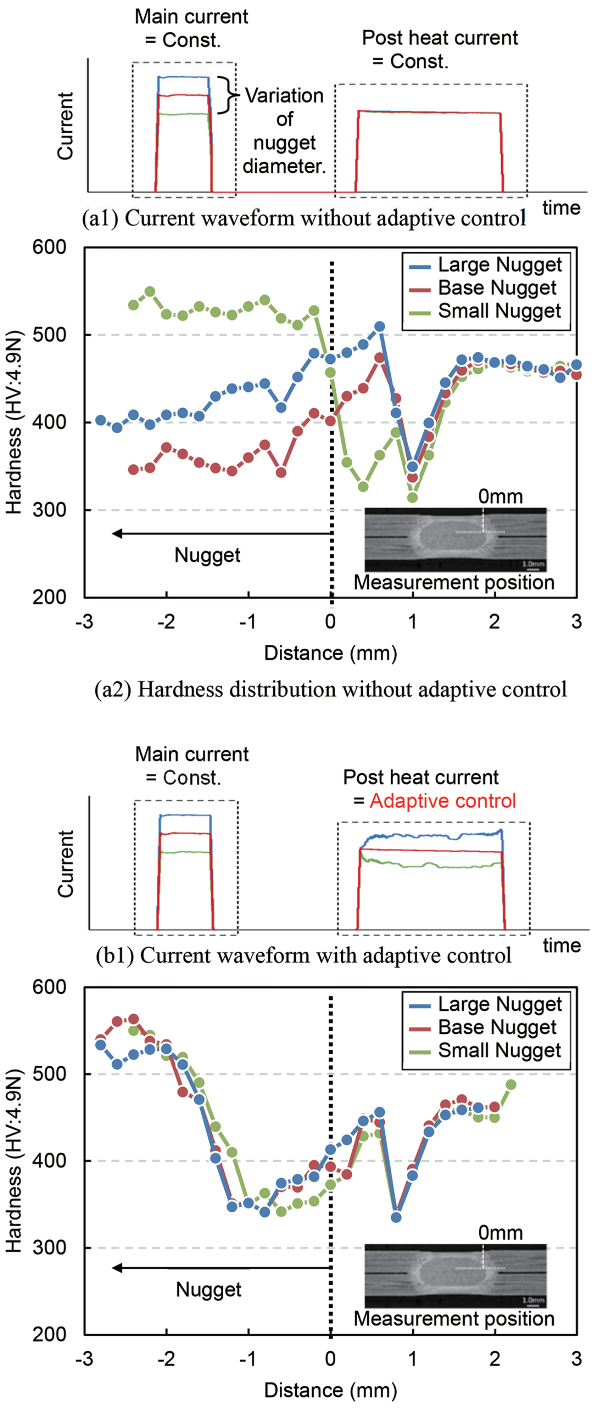

(a1) Current waveform without adaptive control

(a2) Hardness distribution without adaptive control

(b1) Current waveform with adaptive control

(b2) Hardness distribution with adaptive control

Fig. 5 Current waveform and hardness distribution of spot welds after post-heating

baseline condition ($4\sqrt{t}$), the spot-welded joint fractured before the maximum load was reached. In contrast, under all countermeasure conditions, joint fracture occurred after the maximum load, resulting in increased maximum load. In particular, under the combined spot + laser welding condition, the laser welds suppressed buckling between spot welds, further increasing maximum load. Although not shown, the adaptive-control post-heating condition achieved a maximum load comparable to that of the $5\sqrt{t}$ condition, while suppressing spot-weld fracture until the late stage of crushing even at $4\sqrt{t}$.

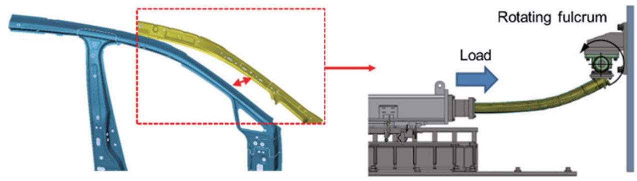

Fig. 6 Schematic diagram of crush test of A-pillar

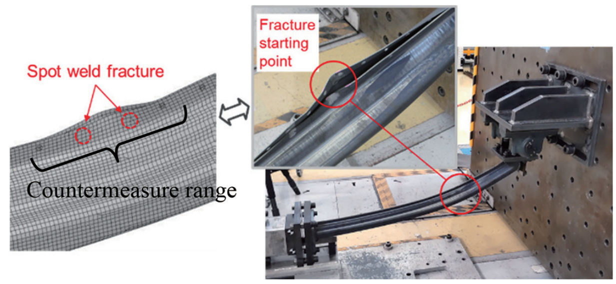

Fig. 7 Result of crush test and spot weld fracture prediction in standard assembly condition

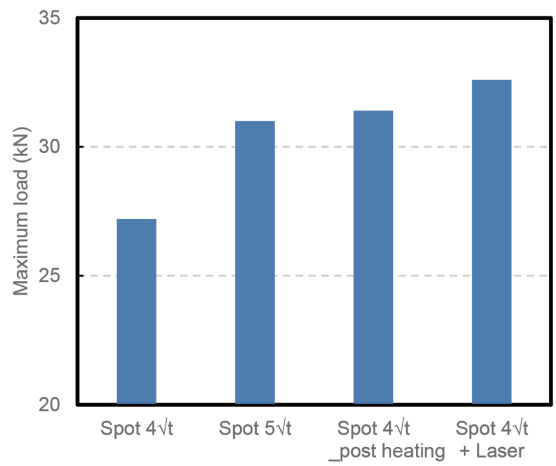

Fig. 8 Comparison of maximum loads under various assembly conditions

The improved margin against spot-weld fracture achieved by adaptive-control post-heating and the increased maximum load due to buckling suppression in the combined spot + laser welding condition suggest that target performance can be achieved even if base-material strength is further increased or section geometry is modified to raise member strength—for example, enabling improved driver visibility by reducing A-pillar width.

Thus, high-accuracy fracture prediction enables performance improvement with minimal countermeasure area. Moreover, under combined spot + laser welding, limiting the countermeasure area also helps mitigate dimensional-accuracy issues caused by thermal distortion, which becomes a concern as laser weld length increases.

5. Conclusion

To achieve high-performance automobile bodies under increasingly stringent crash requirements, it is essential to fully utilize the capability of high-strength steel sheets. Preventing fracture of spot-welded joints is therefore a key technology. This report outlined spot-weld fracture countermeasure processes and presented component-level verification results based on fracture predictions obtained with NSafe™-SPOT. Although some countermeasures may increase tact time and cost relative to conventional spot welding, optimizing their application locations through high-accuracy fracture prediction can minimize such increases. This approach contributes to the development of automobile bodies with an excellent balance between fracture resistance and crash performance.

To meet progressively higher functionality requirements, it is crucial to continue proposing low-cost, highly reliable components by extending beyond material technologies to include production processes and part geometry. We will continue to contribute to automobile body development by realizing reliable joints and proposing new joining processes and methods.

References

1) Kubo, M. et al.: Proceedings of the JSAE Annual Congress. (64-22), 20225281 (2022)
2) Fujimoto, H.: Welding Technology. 70 (3), 38–43 (2022)
3) Yoshida, H. et al.: Proceedings of the JSAE Annual Congress. (8-04), 20045205 (2004)
4) Yoshida, H. et al.: Proceedings of the JSAE Annual Congress. (49-05), 20055062 (2005)
5) Uenishi, A. et al.: Shinnittetsu Giho. (393), 32–38 (2012)
6) Yoshida, H. et al.: Proceedings of the JSAE Annual Congress. (21-07), 20075067 (2007)
7) Furusako, S. et al.: Nippon Seitetsu Giho. (412), 67–77 (2019)
8) Sugino, H.: Journal of the Japan Welding Society. 89 (1), 45–50 (2020)
9) Hamatani, H. et al.: Preprints of the National Meeting of JWS. (89), 44–45 (2011)
10) Hiratsuka, K. et al.: Journal of the Japan Welding Society. 39 (3), 145–155 (1970)
11) Cretteur, L., Merdji, Y., Kaczynski, C.: 7th International Conference on Hot Sheet Metal Forming of High-Performance Steel. CHS2, 385–393 (2019)
12) Taniguchi, T. et al.: Preprints of the National Meeting of JWS. (107), 66–67 (2020)
13) Sakamoto, T. et al.: Preprints of the National Meeting of JWS. (115), 54–55 (2024)

Tohru OKADA
Ph.D., Senior Manager, Head of Section
Welding & Joining Research Lab.
Steel Research Laboratories
20-1 Shintomi, Futtsu City, Chiba Pref. 293-8511

Hiroshi HORIKAWA
Senior Researcher
Welding & Joining Research Lab.
Steel Research Laboratories

Taiga TANIGUCHI
Researcher
Welding & Joining Research Lab.
Steel Research Laboratories

Takumi MIZUTANI
Welding & Joining Research Lab.
Steel Research Laboratories

Junichiro SUZUKI
Quality Management Div.
Nagoya Works

Takahiro AITO
Senior Researcher
Integrated Steel-Solution Research Lab.-I
Steel Research Laboratories

Masatoshi TOKUNAGA
Senior Manager, Head of Section
Welding & Joining Research Lab.
Steel Research Laboratories

Hiroki FUJIMOTO
Ph.D., General Manager, Head of Dept.
Welding & Joining Research Lab.
Steel Research Laboratories

Hiroshi YOSHIDA
Ph.D., General Manager, Head of Div.
Welding & Joining Research Lab.
Steel Research Laboratories